COMPARISON OF INLINE HOT SPOT DETECTION AND EVALUATION ALGORITHMS FOR CRYSTALLINE SILICON SOLAR CELLS

S. Wasmer[1], I. Geisemeyer[1], D. Pfengler[2], J.M. Greulich[1], S. Rein[1]

[1]Fraunhofer Institute for Solar Energy Systems ISE, Heidenhofstr. 2, 79110 Freiburg, Germany
[2]InfraTec GmbH Infrarotsensorik & Messtechnik, Gostritzer Str. 61-63, 01217 Dresden, Germany
Phone: +49 761 - 4588 5075; e-mail: sven.wasmer@ise.fraunhofer.de

ABSTRACT: We present a detailed comparison of five inline-feasible hot spot detection and evaluation algorithms that are tested at the hands of inline thermography measurements of 108 industrial monocrystalline silicon solar cells. We evaluate the algorithms concerning their ability to predict the measured equilibrium temperature increases of the reversely-biased solar cells from short-term measurements and compare the requirements of each method. Beyond that, we apply and test for the first time a novel approach using the temporal evolution of the temperature of a hot spot right after turning on a direct voltage, only needing a series of temperature-calibrated thermography images (time series approach). We show that with the most accurate method of iterative convolution of power-calibrated thermography images with temperature response functions, equilibrium temperature increases can be predicted with a mean absolute error of only 3 K and a correlation coefficient of 0.90. Furthermore, relying both on similar physical considerations, we find the new time-series approach and the temperature increase $T(100 \text{ ms})$-$T(80 \text{ ms})$ in the short-term measurement to yield almost as accurate results (correlation coefficients of 0.86 and 0.87 respectively and mean absolute error of 3.5 K for the time series approach), while implementation is less challenging for these.
Keywords: Silicon Solar Cell, Characterisation, Hot Spot, Reliability, Thermography

1 INTRODUCTION

If a solar cell in a solar module operating in the field is fully or partially shaded, it can be reverse-biased by the other cells in the same string of the module. This is not harmful for usual voltage ranges unless the shaded cell contains breakdown channels. In this case, localized currents can lead to a significant heating of the cell, also referred to as "hot spot", which can eventually irreversibly damage the module components [1, 2]. According to TUV Rheinland, in a global study for the period between 2011 and 2013, almost 6% of 6200 tested modules were sorted out due to hot spot danger [3]. Being able to reliably detect dangerous cells inline after the cell process or prior to module fabrication, while not sorting out too many harmless cells, would be beneficial concerning the yield and quality of production lines. However, since hot spots are often localized, global criteria such as the current I_{rev} at a fixed reverse testing voltage V_{rev} often fail. In contrast, thermography imaging is capable of detecting the local heat dissipation, but it was shown that local short-term temperature increases only weakly correlate with the equilibrium temperature increases $\Delta T_{eq.}$ [4].

As of today, these issues seem not to be resolved and inline hot spot detection and evaluation is not yet common in solar cell production. Furthermore, publications on inline hot spot evaluation algorithms and their reliability are scarce [5, 6]. In this work, we aim for a reliable and relevant hot spot detection method. For this purpose, we compare five algorithms concerning their ability to predict $\Delta T_{eq.}$ of about 100 industrial silicon aluminium back-surface field solar cells with the help of inline measurements and analysis times in the range of 100 ms.

As pointed out above, still many modules do not pass hot spot tests. Furthermore, with the introduction of novel and more complex cell concepts that are possibly more prone to high breakdown currents as well as the potential future increase of the number of cells per string in a module, raising the potential reverse bias applied to a shaded cell, hot spots and their evaluation are still an important topic in inline cell characterisation.

To the authors' knowledge, this is the first systematic comparison of different methods on a statistical basis. Beyond that, we apply and test for the first time a novel approach using the temporal evolution of the temperature of a hot spot right after turning on a direct voltage, only needing a series of temperature-calibrated thermography images (see Sec. 2.2).

2 APPROACH

2.1 Overview

We make use of an uncooled "VarioCAM® hr head" microbolometer camera installed in a "PV-LIT" inline measurement tool from InfraTec incorporated in the cell tester at the "PV-TEC" lab at Fraunhofer ISE. For each of the cells that are mounted in air during the measurement, we first acquire a series of 5 images with a framerate of 50 Hz ("short-term") and second a series of 50 images with an image acquisition frequency of 1 Hz ("equilibrium"). From the equilibrium measurement, we deduce the equilibrium temperature increase $\Delta T_{eq.}$, which we then try to predict solely from the short-term measurements. The system is synchronized such that the time of application of the constant reverse voltage V_{rev} is equal to the start of the image acquisition which is carried out line-by-line, that is the lines of the first image T_{20ms} are acquired corresponding to points in time of 0 to 20 ms after reverse-biasing. Based on the distinct temporal evolution of the temperature of a hot spot, we make use of a novel approach to extract its physical parameters that can be used to predict $\Delta T_{eq.}$. We then determine the correlations between the measured $\Delta T_{eq.}$ with the following methods:

1) Global current $I_{rev}(V_{rev} = -12 \text{ V})$.
2) Temperature increase $\Delta T_{100\leftrightarrow20} = T_{100ms} - T_{20ms}$ in the short-term measurement. We use this to represent a temperature difference $\Delta T_{100\leftrightarrow0}$ with an image T_{0ms} acquired before biasing as with our line-by-line

reading camera, the lines of an image $\Delta T_{100\leftrightarrow0}$ would correspond to significantly different durations of biasing.

3) Temperature increase $\Delta T_{100\leftrightarrow80}$ in the short-term measurement.
4) Predicted temperature increase by our time series approach (see Sec. 2.1).
5) Approach based on the iterative convolution of power-calibrated thermography images with temperature response functions, as described in Ref. [7]. We use power-calibrated $\Delta T_{100\leftrightarrow20}$ images for this end.

We test the methodologies at the hands of measurements of 108 industrial monocrystalline silicon solar cells that apart from hot spots show homogeneous electrical properties. We conduct the measurements using a reverse voltage of $V_{rev} = -12$ V and acquire two time series of thermography images with the uncooled microbolometer camera: firstly with an image acquisition frequency of 50 Hz for 100 ms in order to garner the temporal evolution of the hot spots right after application of the direct voltage and secondly with 1 Hz for 50 s, which proves to be enough to reach equilibrium and determine the resulting temperature increase $\Delta T_{eq.}$. We then analyse the correlations between $\Delta T_{eq.}$ with each of the methods given above. Before illustrating the results of that comparison, we first give in the next section a short review of the methodology of the time series approach.

2.2 Time-series approach

If a solar cell with diode breakdown channels is reversely biased, current flowing through these channels can lead to a significant local heating of the solar cell, also referred to as the term "hot spot". The temporal evolution of this heating in the range of milliseconds to seconds right after applying the reverse bias can reveal important physical properties of the examined hot spot [8]. The simulations are carried out by an analytical model, where a hot spot is assumed to be a cylindrical breakdown channel with radius r_0 and power P_{in}, spanned over the whole cell thickness. The boundary conditions of convection and radiation are considered to be negligible on these short time scales. The temperature increase distribution $\Delta T(r,t)$ depends on time t and distance r from the hot spot origin (in cylindrical coordinates). $\Delta T(r,t)$ can be calculated (see also Ref. [9]) as:

$$\Delta T(r,t;P_{in},r_0) = \frac{4P_{in}}{\pi^3 r_0^3 dk} \int_0^\infty \left(1 - e^{-\kappa u^2 t}\right) \cdot \frac{J_0(ur) \cdot J_1(ur_0)}{u^4(J_1(r_0 u)Y_0(r_0 u) - J_0(r_0 u)Y_1(r_0 u))^2} \, du \quad (1)$$

with J_n and Y_n the Bessel functions of the first and second kind of order n, d the cell thickness and k and κ denote the thermal conductivity and diffusivity of silicon.

By applying this result, we first acquire a series of thermography images right after the application of the reverse bias. We then adjust the analytical model to fit the measured temporal evolution of the hottest pixel on the cell and extract its characteristic parameters P_{in} and r_0. These can then be mapped to an expected equilibrium temperature increase $\Delta T_{eq.}$ with a look-up table, allowing to evaluate the possible danger of a cell prior to module production in the range of 100 ms for the measurement

and 10 ms for the analysis, suitable for inline application. This approach using a time series of thermography images is further illustrated and explained in Figure 1, where we depict the measurement and simulation of the time-dependent temperature evolution of a) a hot spot in the cell area and b) a hot spot in the corner of a silicon solar cell after the application of a reverse voltage at time $t = 0$ s. Temperatures are shown for the hottest pixel, measured with the uncooled microbolometer camera with a resolution of 355 µm per pixel and a framerate of 50 Hz.

Given are the best fits of r_0 and P_{in} to match the measurement data until 0.1 s (first 5 frames, dashed line) and until 1 s (all 50 frames, full line). For both hot spot sites, our analytical model can well describe the temporal evolution of the hot spot, with only slight relative deviations (+5% and -11%) in case of extrapolating the
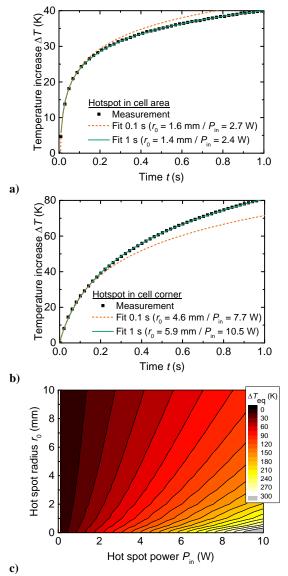

a)

b)

c)

Figure 1: Short-term measurement and simulation of the time-dependent temperature evolution of the hottest pixel of **a)** a hot spot in the cell area and **b)** a hot spot in the corner of a silicon solar cell.
c) Numerically simulated equilibrium temperature increases that the camera would measure if the hot spot origin would lie in the centre of a pixel.
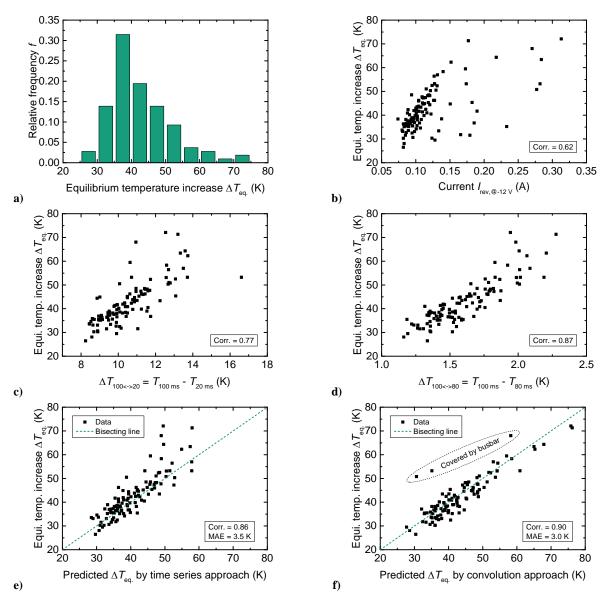
Figure 2: a) Histogram of the measured equilibrium temperature increase of the hottest pixels of the 108 silicon solar cells. Correlation plots of the measured equilibrium temperature increase $\Delta T_{eq.}$ with

b) the global reverse current $I_{rev}(V_{rev} = -12 \text{ V})$,

c) the measured temperature increase $\Delta T_{100 \leftrightarrow 20}$ in the short-term measurement,

d) the measured temperature increase $\Delta T_{100 \leftrightarrow 80}$ in the short-term measurement,

e) predicted temperature increase by our introduced "time series approach" and

f) the approach based on the iterative convolution of power-calibrated thermography images with temperature response functions [7] (using power-calibrated $\Delta T_{100 \leftrightarrow 20}$ images). Parts of the signal of the hot spots of the three marked points were covered by busbars, which introduces a large deviation.

fit from the first 5 to all 50 measurement points, i.e. from 0.1 s to1 s.

In c) the resulting equilibrium temperature increase by numerical simulations for a broad variation of r_0 and P_{in} and assuming a convection coefficient of $h_{conv} = 8 \text{ W/(m}^2\cdot\text{K)}$ and an emissivity of 0.9 on both sides is depicted. Given are the temperatures that the camera would measure if the hot spot origin would lie in the centre of a circular cell with radius of 15.6/2 cm that is mapped to the centre of a pixel. These simulations serve as a look-up table for our time series approach, where first r_0 and P_{in} are extracted from the temporal evolution of the hot spot temperature and which then are converted to a prediction of the equilibrium temperature.

As an intermediate result, we find our analytical model to describe the temporal evolution of the temperature of a hot spot right after switching on the reverse voltage to be well suited to fit our measurements. Fundamentally, the signal-to-noise ratio of the thermography images seems to be high enough to analyse the time-dependent temperature development even on the pixel level.

3 RESULTS

The measured equilibrium temperature increases ΔT_{eq} are given in Figure 2(a) and lie within 26 to 72 K with a

median of 40 K, and the comparison of the correlations of the five tested hot spot detection and evaluation methods with ΔT_{eq} are given in Figure 2(b-f).

Concerning our approach based on the temporal evolution of hot spot temperatures, we find the hot spot radii to lie within 1.3 to 4.5 mm with a peak at 3.4 mm and hot spot powers of 1.5 to 3.7 W, with most being around 2.3 W. Note that these hot spot powers significantly exceed the global powers $V_{rev} \cdot I_{rev}$, which is due to the fact that almost all hot spots happen to be located at the cells' edges or corners. Within the time series approach, the increased apparent hot spot powers due to the mirroring of heat waves at the cells' edges are inherently correctly included (in the convolution approach, this has to be taken care of explicitly).

Regarding the approach based on the iterative convolution with temperature response functions, we calibrate temperature difference images $\Delta T_{100\leftrightarrow20}$ with a calibration factor of 0.00073 W/K.

Concerning methods 4) and 5), we find a convection coefficient of $h_{conv} = 8$ W/(m²·K) to describe most accurately the cooling conditions in the measurement chamber of our inline cell tester during the measurements.

Finally, we find Pearson correlation coefficients of $\rho = 0.62$ for the global criterion of the current I_{rev} as well as 0.77 and 0.87 for the short-term temperature increases $\Delta T_{100\leftrightarrow20\,ms}$ and $\Delta T_{100\leftrightarrow80}$, respectively. The more advanced methods of time series and convolution approach exhibit $\rho = 0.86$ and 0.90 with mean absolute errors MAE = 3.5 and 3.0 K.

4 DISCUSSION

Concerning the correlation analysis for the measured equilibrium temperatures increases ΔT_{eq}, we expectedly identify the global criterion of the current I_{rev} and the short-term temperature increase $\Delta T_{100\leftrightarrow20}$ to show only weak prediction accuracies.

We obtain significantly more accurate results for the more advanced approaches, namely the newly introduced time series approach and the convolution method. Our results show that both evaluation algorithms can be utilized to predict ΔT_{eq} accurately enough based on inline-feasible measurements that last only 100 ms.

Table I: Tentative comparison of the requirements and prediction accuracies of the five hot spot evaluation algorithms.

	Number of images	Precision of synchronisation	Simplicity of calibration	Complexity of image processing	Prediction accuracy of ΔT_{eq}
1) $I_{rev}(V_{rev} = -12$ V$)$	0	++	++	++	--
2) $\Delta T_{100\leftrightarrow20}$	2	0	+	+	-
3) $\Delta T_{100\leftrightarrow80}$	2	-	+	+	0
4) Time series	4	--	-	0	+
5) Convolution	2	0	--	--	++

However, they still can fail on certain occasions, as we find maximal deviations of -18.8 K and -20.2 K for the time series and convolution approach respectively. We explain most of the outliers to be due to superposed heat flux of accumulated hot spots in the vicinity to each other, not detectable by the time series approach in the short-term measurement. In case of the convolution approach, we find all three severe outliers to be caused by busbars shading parts of the power signal.

Interestingly, the tested method 3), that is the temperature increase $\Delta T_{100\leftrightarrow80}$ in the short-term measurement, shows a significantly better correlation than that of the temperature increase $\Delta T_{100\leftrightarrow20}$, although exhibiting much lower absolute signals that are more prone to noise. An explanation for this is that according to the findings in Ref. [8] and Eq. (1), the most important characteristic of hot spot power P_{in} is weaker correlated to the absolute temperature increase $T(t_1)-T(t_0 \approx 0$ ms$)$ than to the difference between the temperatures at two time points t_0 and t_1, with t_0 considerably greater than zero.

As these results are achieved on cell level, care has to be taken while transferring these results on module level. This could be done by changing the look-up table in Figure 1(c) for the time series approach and the point spread functions of the convolution approach (Ref. [7]) to those of the applied module layout. However, as we believe that there is a strong correlation between the measured $\Delta T_{eq,cell}$ of cells mounted in air with the measured $\Delta T_{eq,module}$ at the backsheet of the finished module, an empirical, monotonous relation $\Delta T_{eq,module}(\Delta T_{eq,cell})$ could be found experimentally.

4.1 Comparison of requirements

In order to enable a better assessment of the requirements of the different methods, we give in Table I an overview of the requirements categorized in 5 classes based on our experiences, ranging from "--" (difficult to implement) to "++", meaning basically no effort has to be put into. Approach 1), that is the global current, has of course the least restrict requirements, however, the use for predicting ΔT_{eq} is rather minimal. Better in this respect are the temperature increases in the short-term measurements 2) and 3), with $\Delta T_{100\leftrightarrow80}$ being more reliable albeit posing more problems concerning the synchronization as two images within a distinct time interval after applying the reverse voltage are needed, contrary to one image before, where the exact timestamp is irrelevant, and one image after biasing. We have to note that here both images $\Delta T_{100\leftrightarrow20}$ and $\Delta T_{100\leftrightarrow80}$ are calculated from images after biasing, while the first is actually used to represent a temperature difference $\Delta T_{100\leftrightarrow0}$ with an image T_{0ms} acquired before biasing, see also Sec. 2.1, bullet point 2), which should be easier to implement.

Better prediction results can be achieved with the methods 4) and 5), referred to as time series and convolution approach, which also are the only ones that give direct predictions of ΔT_{eq} in units of K. By utilizing 4), however, more difficulties arise, as at least 4 temperature-calibrated thermography images perfectly synchronized in equidistant time steps have to be acquired and analysed. Concerning 5), calibration is even more restrained as power-calibrated short-term thermography imaging measurements are needed. Furthermore, the edges of the cell in the image have to be

known in order to mirror the power sources before the challenging image processing step of convolution with temperature response functions. Both of the advanced methods furthermore need numerical simulations to calculate the expected equilibrium temperature increases and the temperature response functions respectively as well as require a one-time calibration of the convection coefficient to the cooling conditions of the measurement chamber.

5 SUMMARY AND CONCLUSION

We compared five hot spot detection and evaluation algorithms concerning their ability to predict the equilibrium temperature increase ΔT_{eq} of reversely biased silicon solar cells and as well assessed their hard- and software requirements. The methods were tested at the hands of about 100 industrial silicon solar cells using inline-feasible measurements and analyses.

We found the highest prediction accuracy with a mean absolute error of only 3 K to be possible with the approach based on the convolution of power-calibrated thermography images. While it is the physically soundest approach and especially outperforms the others in case of planar or many local hot spots in the vicinity of each other, inline feasibility is still given.

Our newly introduced algorithm based on the analysis of the temporal evolution of hot spot temperatures was a bit less accurate (mean absolute error 3.5 K), while implementation is somewhat less challenging. Using the same physical background as for this time series approach, we identified the temperature increase $\Delta T_{100 \leftrightarrow 80}$ in the short-term measurement to show quite a good correlation of $\rho = 0.87$ with the reference ΔT_{eq}, thus representing a good compromise between prediction accuracy and requirements.

The comparison conducted in this work lays ground for reliable classification algorithms of hot spots, where the next step of transfer to module level can be easily carried out. Then, the critical equilibrium temperature increase $\Delta T_{eq.,critical}$ has to be defined depending on the module layout and mounting location as well as different shading scenarios.

Despite that, $\Delta T_{eq.,critical}$ can be tuned for a trade-off of quality and yield of the sorting algorithm, for example using its receiver operating characteristic curve.

ACKNOWLEDGEMENT

REFERENCES

[1]   F. Fertig, S. Rein, M. C. Schubert, and W. Warta, "Impact of Junction Breakdown in Multi-Crystalline Silicon Solar Cells on Hot Spot Formation and Module Performance," in *26th EUPVSEC Hamburg*, 2011, pp. 1168–1178.

[2]   I. Geisemeyer, F. Fertig, W. Warta, S. Rein, and M. C. Schubert, "Prediction of silicon PV module temperature for hot spots and worst case partial shading situations using spatially resolved lock-in thermography," *Solar Energy Materials and Solar Cells*, vol. 120, pp. 259–269, http://www.sciencedirect.com/science/article/pii/S0927024813004856, 2014.

[3]   G. TamizhMani *et al., Eds., Regional influence on module design quality: Qualification testing failure rate results from six regional labs of TUV rheinland around the world*. IEEE 40th Photovoltaic Specialist Conference (PVSC), 2014.

[4]   T. Roth, R. Siebert, and K. Meyer, "From Short-term Hotspot Measurements to Long-term Module Reliability," *Energy Procedia*, vol. 55, pp. 504–508, 2014.

[5]   J. Hudson, L. Vasilyev, J. Schmidt, and G. Horner, Eds., *Economic impacts and approaches to address hot-spot defects in photovoltaic devices*. 35th IEEE Photovoltaic Specialists Conference, 2010.

[6]   K. Ramspeck, S. Schenk, D. Duphorn, A. Metz, and M. Meixner, "In-line thermography for reliable hot spot detection and process control," *Energy Procedia*, vol. 55, pp. 133–140, 2014.

[7]   I. Geisemeyer, F. Fertig, W. Warta, S. Rein, and M. C. Schubert, "Fast Hot Spot Evaluation," in *29th EUPVSEC Amsterdam*, Amsterdam, The Netherlands, 2014, pp. 2429–2434.

[8]   S. Wasmer et al., "Analytical modelling of the temporal evolution of hot spot temperatures in silicon solar cells," to be published.

[9]   H. S. Carslaw and J. C. Jaeger, *Conduction of heat in solids,* 2nd ed. Oxford [Oxfordshire], New York: Clarendon Press; Oxford University Press, 1986, ©1959.